

Characteristics of Multilayered Metamaterial Structures Embedded in Fractional Space for Terahertz Applications

Safiullah K. Marwat^{1, *} and Muhammad J. Mughal^{1, 2}

Abstract—This paper discusses the electromagnetic characteristics of a stratified metamaterial structure placed in fractional dimension space. Reflection and transmission coefficients for plane wave incident on multilayered structure in D -dimensional space are computed. Transfer matrix method is used to study the behaviour of different planer multilayered periodic metamaterial structures. The results are compared for integer and fractal dimensional spaces for both the cases of normal and oblique incidences. Classical results are recovered for integer dimensions. This work provides solution for examining the electromagnetic fields and waves in multilayered structures at fractal interfaces.

1. INTRODUCTION

To achieve desired electromagnetic characteristics, multilayered structures are formed by combining slabs composed of materials having special properties. These structures are used in anti-reflection coatings, radar absorbing structures, and filters [1–3]. Alternating layers of double positive (DPS) and double negative (DNG) materials are used to show transmission tunneling [4]. Liu and Behdad demonstrated that the problem of EM wave tunneling through cascaded epsilon-negative metamaterial and double positive material barrier structure is analogous to the classical problem of coupled-resonator microwave filters [5]. In recent studies on multilayered structures, researchers have been using integer dimension substrate [1–6, 21]; this means that the effect of dimension on the characteristics of structures was not considered. This research has been carried out to further include the parameter of dimension and see its effect on the characteristics of the multilayered structures, because not every object that exists in this universe can be modeled with Euclidean geometry (integer dimension). Shapes and structures with irregular and rough geometry are categorized as fractal media. For instance, coastlines, porous media, cracks, turbulent flows, clouds, mountains, lightning bolts, brain, snowflakes, melting ice, and other systems at phase transitions [7]. The concept of fractal was first introduced by Mandelbrot [8]. There are so many fractal media around us that a book “Fractals Everywhere” appears in literature [9]. Therefore, a solution in D dimension space is required to understand the behaviour of the structures. Lately, solutions to plane wave, differential electromagnetic (EM) wave, cylindrical wave and spherical wave in D -dimension fractional space are developed by Zubair et al. [10–13]. Since then much work has been done on the propagation of waves in fractional dimension space [14–19]. Hence, complex structures can now be modeled with an exact solution.

Therefore in this paper, characteristics of stratified metamaterials (MTMs) placed in fractional dimension space is discussed when an EM plane wave propagates through it. MTMs are synthetic materials that are artificially designed to achieve desired material properties. Chiral (CH) material have the property of non-superposable to their mirror image. Material having permittivity and permeability simultaneously zero (for certain range of frequency) and chirality non-zero are termed

Received 6 November 2013, Accepted 16 January 2014, Scheduled 27 January 2014

* Corresponding author: Safiullah Khan Marwat (safiullah.khan@hotmail.com).

¹ Faculty of Electronic Engineering, GIK Institute of Engineering Sciences and Technology, Topi, Swabi, Khyber Pakhtunkhwa 23640, Pakistan. ² Department of Electrical Engineering, COMSATS Institute of Information Technology, Islamabad, Pakistan.

as chiral nihility (CN). Materials with chirality to refractive index ratio greater than 1 are called strong chiral materials(SC) [20].

In Section 2, the layout of the structure and its associated parameters are explained. In Section 3, analytical derivation of the reflection from and transmission through multilayered MTM structure using transfer matrix method (TMM) is presented. Expressions for incident, reflected and transmitted fields are computed. These expressions are valid for D dimension space ($2 \leq D \leq 3$). In Section 4, numerical results of four cases, CH-CH periodic structure, SC-SC periodic structure, SC-dielectric periodic structure, and CN-CN periodic structure are presented and discussed to study the variation in structure characteristics with changing dimension, frequency and/or incident angle.

2. MULTILAYERED STRUCTURE MODEL

A homogenous structure has odd number of parallel planar slabs of MTMs. The slabs are infinite in length as shown in Figure 1. Slabs at odd places are labeled as A having refractive index n_A and width d_A . The slabs at even position are labeled as B having refractive index n_B and width by d_B . κ is the dimensionless chirality parameter. The chirality parameter brings optical activity, circular dichroism, and polarization rotation to the system [23]. Optical widths of slab A and slab B are expressed as $|n_A|d_A$ and $|n_B|d_B$, respectively. The structure is placed in fractional space having refractive index n_F (refractive index is assumed to be approximately same as that of integer space). Furthermore, fractionality only exists in z -axis. TMM is used to compute the incident, reflected and transmitted plane wave expressions after applying proper boundary conditions on the particular interface.

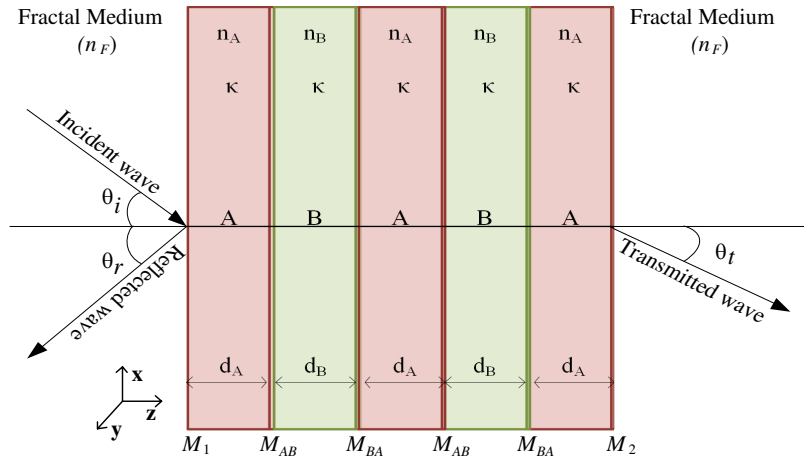


Figure 1. Five layered metmaterial structure placed in fractional dimension space.

3. PROPAGATION EQUATIONS

To compute the field equations for multilayered structure, TMM method is used. A plane wave from fractal medium is incident upon the MTMs at an angle θ_i . The interface is located at $z = 0$. The incident, reflected and transmitted electric and magnetic fields in fractal medium can be written as,

$$\mathbf{E}_i = [E_{i\parallel} (\hat{x} \cos \theta_i + \hat{z} \sin \theta_i) + E_{i\perp} \hat{y}] e^{-jk_F(-x \sin \theta_i)} (k_F z \cos \theta_i)^n \left[H_n^{(2)}(k_F z \cos \theta_i) \right], \quad (1)$$

$$\mathbf{H}_i = \frac{1}{\eta} [E_{i\parallel} \hat{y} - E_{i\perp} (\hat{x} \cos \theta_i + \hat{z} \sin \theta_i)] e^{-jk_F(-x \sin \theta_i)} (k_F z \cos \theta_i)^{nh} \left[H_{nh}^{(2)}(k_F z \cos \theta_i) \right], \quad (2)$$

$$\mathbf{E}_r = [E_{r\parallel} (\hat{x} \cos \theta_r - \hat{z} \sin \theta_r) + E_{r\perp} \hat{y}] e^{-jk_F(-x \sin \theta_r)} (k_F z \cos \theta_r)^n \left[H_n^{(1)}(k_F z \cos \theta_r) \right], \quad (3)$$

$$\mathbf{H}_r = \frac{1}{\eta} [-E_{r\parallel} \hat{y} + E_{r\perp} (\hat{x} \cos \theta_r - \hat{z} \sin \theta_r)] e^{-jk_F(-x \sin \theta_r)} (k_F z \cos \theta_r)^{nh} \left[H_{nh}^{(1)}(k_F z \cos \theta_r) \right], \quad (4)$$

$$\mathbf{E}_t = [E_{t\parallel} (\hat{x} \cos \theta_t + \hat{z} \sin \theta_t) + E_{t\perp} \hat{y}] e^{-jk_F(-x \sin \theta_t)} (k_F z \cos \theta_t)^n \left[H_n^{(2)}(k_F z \cos \theta_t) \right], \quad (5)$$

$$\mathbf{H}_t = \frac{1}{\eta} [E_{t\parallel} \hat{y} - E_{t\perp} (\hat{x} \cos \theta_t + \hat{z} \sin \theta_t)] e^{-jk_F(-x \sin \theta_t)} (k_F z \cos \theta_t)^{nh} \left[H_{nh}^{(2)}(k_F z \cos \theta_t) \right], \quad (6)$$

where i , r and t represent the incident, reflected, and transmitted fields, respectively. Similarly, parallel and perpendicular components of the field are represented by subscripts \parallel and \perp , respectively. The wave number of fractal medium is $k_F = \omega \sqrt{\epsilon \mu}$ and wave impedance $\eta = \sqrt{\frac{\mu}{\epsilon}} = \eta_0 / n_F$. \hat{x} , \hat{y} and \hat{z} are the vectors, and exponential function is used to represent the propagation of the wave in x direction. Hankel function of the second kind is used for forward propagating ($+z$ -axis) wave, and Hankel function of the first kind is used for reverse propagating ($-z$ -axis) wave [14]. The subscripts n and nh define the order of the Hankel function and $n = \frac{|3-D|}{2}$ and $nh = \frac{|D-1|}{2}$ where D is the dimension [15].

The wave incident from fractal medium travels through odd number of chiral MTM slabs. Therefore, a relation between transmitted field in fractal medium and incident field in fractal medium is established, accounting the propagation through chiral slabs. Without loss of generality, the electric and magnetic fields expressions for circularly polarized wave in chiral medium can be written as [21],

$$\mathbf{E}^+ = \mathbf{E}_L^+ \left[e^{-jk_L(z \cos \theta_L - x \sin \theta_L)} \right] + \mathbf{E}_R^+ \left[e^{-jk_R(z \cos \theta_R - x \sin \theta_R)} \right], \quad (7)$$

$$\mathbf{E}^- = \mathbf{E}_L^- \left[e^{-jk_L(-z \cos \theta_L - x \sin \theta_L)} \right] + \mathbf{E}_R^- \left[e^{-jk_R(-z \cos \theta_R - x \sin \theta_R)} \right], \quad (8)$$

where,

$$\mathbf{E}_L^+ = E_L^+ (\hat{x} \cos \theta_L + \hat{z} \sin \theta_L + j\hat{y}), \quad (9)$$

$$\mathbf{E}_R^+ = E_R^+ (\hat{x} \cos \theta_R + \hat{z} \sin \theta_R - j\hat{y}), \quad (10)$$

$$\mathbf{E}_L^- = E_L^- (-\hat{x} \cos \theta_L + \hat{z} \sin \theta_L + j\hat{y}), \quad (11)$$

$$\mathbf{E}_R^- = E_R^- (-\hat{x} \cos \theta_R + \hat{z} \sin \theta_R - j\hat{y}), \quad (12)$$

Similarly [22],

$$\mathbf{H}^+ = \mathbf{H}_L^+ \left[e^{-jk_L(z \cos \theta_L - x \sin \theta_L)} \right] + \mathbf{H}_R^+ \left[e^{-jk_R(z \cos \theta_R - x \sin \theta_R)} \right], \quad (13)$$

$$\mathbf{H}^- = \mathbf{H}_L^- \left[e^{-jk_L(-z \cos \theta_L - x \sin \theta_L)} \right] + \mathbf{H}_R^- \left[e^{-jk_R(-z \cos \theta_R - x \sin \theta_R)} \right], \quad (14)$$

where,

$$\mathbf{H}_L^+ = \frac{-j}{\eta} E_L^+ (\hat{x} \cos \theta_L + \hat{z} \sin \theta_L + j\hat{y}), \quad (15)$$

$$\mathbf{H}_R^+ = \frac{j}{\eta} E_R^+ (\hat{x} \cos \theta_R + \hat{z} \sin \theta_R - j\hat{y}), \quad (16)$$

$$\mathbf{H}_L^- = \frac{-j}{\eta} E_L^- (-\hat{x} \cos \theta_L + \hat{z} \sin \theta_L + j\hat{y}), \quad (17)$$

$$\mathbf{H}_R^- = \frac{j}{\eta} E_R^- (-\hat{x} \cos \theta_R + \hat{z} \sin \theta_R - j\hat{y}), \quad (18)$$

subscripts $+$ and $-$ indicate the fields traveling in forward and backward direction respectively. Wave numbers for left circular polarization (LCP) and right circular polarization (RCP) are,

$$k_g = \omega \sqrt{\epsilon \mu} (1 \mp \kappa_r) \quad g = L, R, \quad (19)$$

where, $\kappa_r = \kappa / \sqrt{\epsilon_r \mu_r}$ and for strong chiral medium $\kappa_r > 1$ [20]. θ_L and θ_R can be computed using snell's law,

$$\theta_g = \left(\frac{k_F \sin \theta_i}{k_g} \right) \quad g = L, R. \quad (20)$$

Dispersion can be observed if permittivity (ϵ) is frequency dependent. In (19) wave number for LCP and RCP waves depends on frequency, which in turn means that the propagation velocity of the wave will

vary with the change in frequency. Moreover, all the permittivity dependent parameters will be affected, i.e., reflection coefficient, transmission coefficient. To determine the reflected and transmitted fields from planar multilayered metamaterial structure transfer matrix method is used. Firstly, boundary conditions are applied to form a matching matrix that relates the fields on either side of the interface. Secondly, propagation matrices are constituted to determine the forward and backward field propagations in slabs. Lastly, a transition matrix is constructed using matching and propagation matrices.

Consider M_1 interface that is located between fractal medium and slab A as shown in Figure 1. Applying proper boundary conditions on (1)–(4), (7)–(8) and (13)–(14), four linear equations are obtained. These equations are rearranged and presented,

$$= \begin{bmatrix} H_{2e} \cos \theta_i & 0 & -H_{1e} \cos \theta_r & 0 \\ 0 & H_{2e} & 0 & -H_{1e} \\ 0 & -n_F H_{2h} \cos \theta_i & 0 & -n_F H_{1h} \cos \theta_r \\ n_F H_{2h} & 0 & n_F H_{1h} & 0 \end{bmatrix} \begin{bmatrix} E_{i\parallel} \\ E_{i\perp} \\ E_{r\parallel} \\ E_{r\perp} \end{bmatrix} \\ = \begin{bmatrix} \cos \theta_L & \cos \theta_R & \cos \theta_L & \cos \theta_R \\ j & -j & -j & j \\ -n_A j \cos \theta_L & n_A j \cos \theta_R & -n_A j \cos \theta_L & n_A j \cos \theta_R \\ n_A & n_A & -n_A & -n_A \end{bmatrix} \begin{bmatrix} E_L^+ \\ E_L^- \\ E_R^+ \\ E_R^- \end{bmatrix}, \quad (21)$$

where,

$$H_{1e} = (k_F z \cos \theta_r)^n \left[H_n^{(1)}(k_F z \cos \theta_r) \right], \quad (22)$$

$$H_{2e} = (k_F z \cos \theta_i)^n \left[H_n^{(2)}(k_F z \cos \theta_i) \right], \quad (23)$$

$$H_{1h} = (k_F z \cos \theta_r)^{nh} \left[H_{nh}^{(1)}(k_F z \cos \theta_r) \right], \quad (24)$$

$$H_{2h} = (k_F z \cos \theta_i)^{nh} \left[H_{nh}^{(2)}(k_F z \cos \theta_i) \right], \quad (25)$$

substituting (22)–(25) in (21) and applying simple matrix multiplication M_1 is obtained.

$$\begin{bmatrix} E_{i\parallel} \\ E_{i\perp} \\ E_{r\parallel} \\ E_{r\perp} \end{bmatrix} = [M_1] \begin{bmatrix} E_L^+ \\ E_L^- \\ E_R^+ \\ E_R^- \end{bmatrix}. \quad (26)$$

In a similar manner M_2 , M_{AB} and M_{BA} can be computed. A propagation matrix for a slab having width equal to d_s ($s = A, B$) and wave number k_i ($i = L, R$) can be written as,

$$P_A = \begin{bmatrix} e^{-jk_L d_A} & 0 & 0 & 0 \\ 0 & e^{-jk_R d_A} & 0 & 0 \\ 0 & 0 & e^{jk_L d_A} & 0 \\ 0 & 0 & 0 & e^{jk_R d_A} \end{bmatrix} \quad (27)$$

$$\begin{bmatrix} E_{i\parallel} \\ E_{i\perp} \\ E_{r\parallel} \\ E_{r\perp} \end{bmatrix} = T \begin{bmatrix} E_{t\parallel} \\ E_{t\perp} \end{bmatrix} \quad (28)$$

where T is the 4×2 transition matrix which relates the total field on one side of the structure to the fields on the other side.

$$T = [M_1][P_A][T_1]^m[M_2] \quad (29)$$

$$T_1 = [M_{AB}][P_B][M_{BA}][P_A] \quad (30)$$

The expressions are valid for any odd number of slabs ($2m + 1$, where m is a positive integer). In (30), $[M_{AB}]$ and $[M_{BA}]$ are 4×4 matching matrices, and $[P_B]$ and $[P_A]$ are propagation matrices for slab B and slab A , respectively. Furthermore, In (29) matching matrix $[M_1]$ is a 4×4 matrix whilst $[M_2]$ is a 2×4 matrix.

All equations derived are for non-integer dimension space. Insertion of integer dimension (i.e., $D = 2$) recovers the classical results. In this paper, numerical results of four different cases are presented and discussed. All structures presented consist of five alternating layers (else mentioned), constructing a stack of the form $ABABA$. The structure is embedded in fractional space (non-integer dimension space). Behaviour of structure is analysed for varying slab width (d), chirality (κ), angle of incidence (θ_i), dimension (D) of incident and transmitted medium and frequency. The results for varying dimension are presented in this paper. Note that refractive index of fractal medium is taken as 1.5 in all cases, and λ_0 is the wavelength at 1 THz operational frequency.

4. RESULTS AND DISCUSSION

4.1. CH-CH Structure

In the first case, both slabs A and B are composed of CH MTM with slab A having higher refractive index than slab B . When an EM wave impinges on CH-CH structure at an angle of 60° from a fractal medium, it is partially reflected and partially transmitted. The effect of dimension over the range of frequency can be seen in Figure 2. Figures 2(a) and 2(b) describe the relation between reflected power and frequency. It is observed that increasing dimension of the substrate increases the parallel reflection power and barely decreases perpendicular reflection power. Whereas power transmitted decreases with the increase in dimension D . In Figures 2(c) and 2(d), it can be seen that dimension of the incident medium has significant effect on the transmitted power through the structure. When the dimension of substrate is $2.5D$, the parallel component of transmission is less than 5% after 0.6 THz to the total power transmitted while for $2.0D$ substrate it is 25% approximately. The structure behaves like a pass band

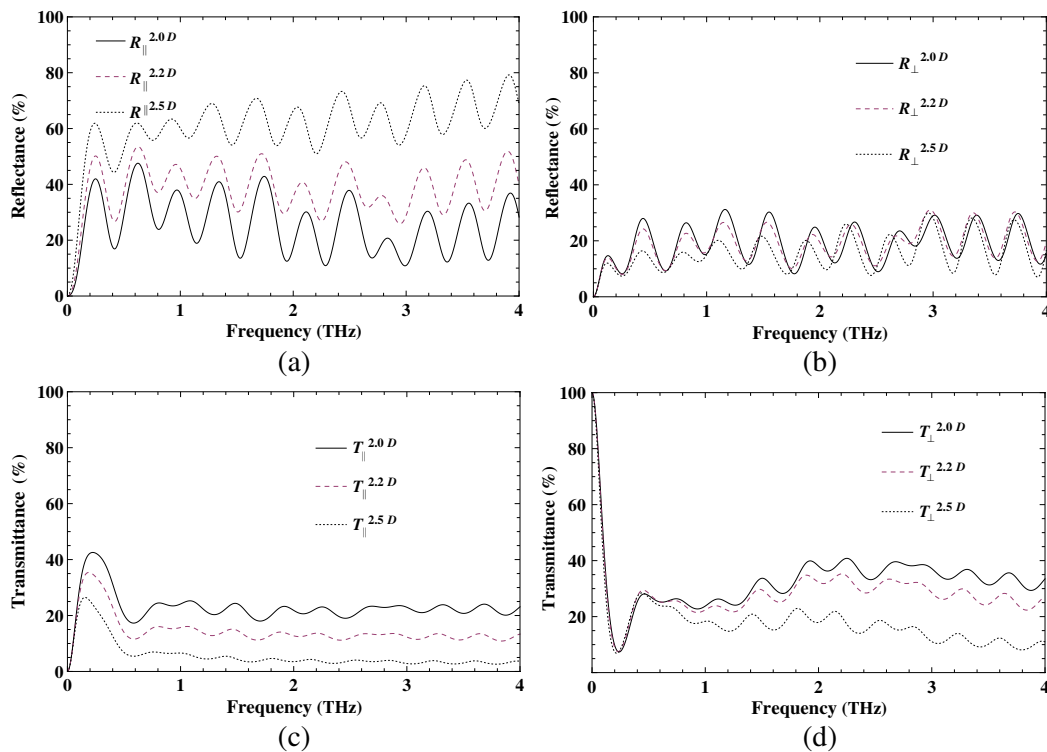


Figure 2. Reflectance and transmittance versus frequency for five layered CH-CH structure. $n_A = 2.6$, $n_B = 1.5$, $\kappa_A = \kappa_B = 0.8$, $|n_A|d_A = |n_B|d_B = \lambda_0/4$, and $\theta_i = 60^\circ$.

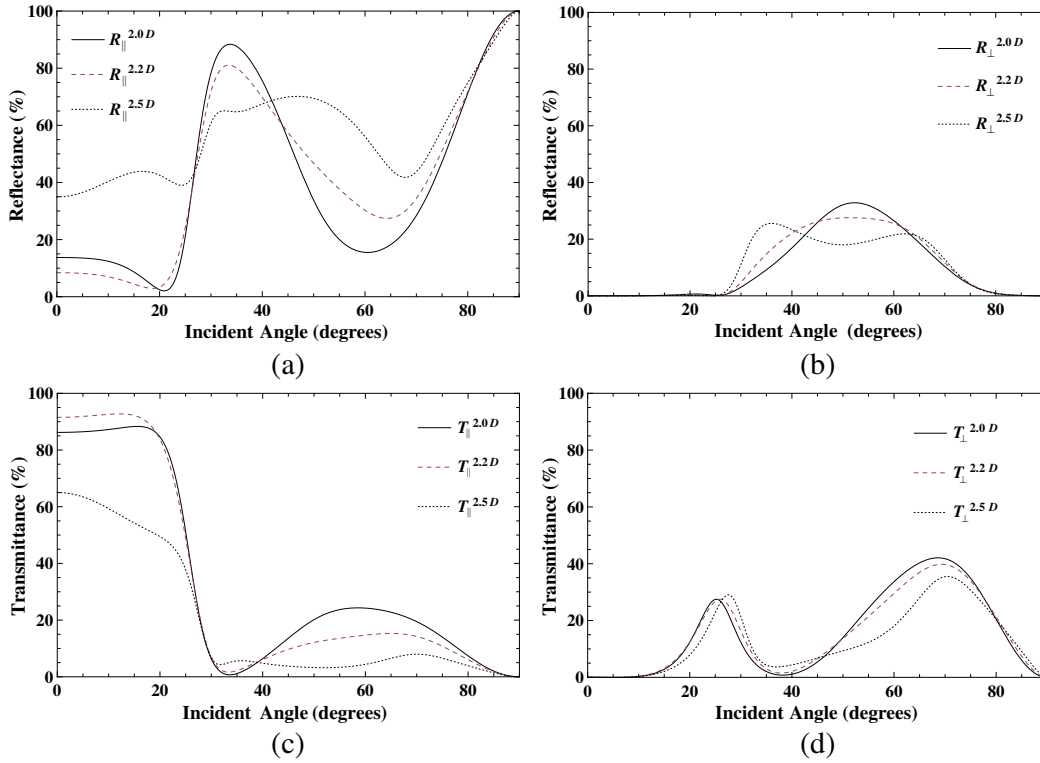


Figure 3. Reflectance and transmittance versus incident angle for five layered CH-CH structure. $n_A = 2.6$, $n_B = 1.5$, $\kappa_A = \kappa_B = 0.8$, $|n_A|d_A = |n_B|d_B = \lambda_0/4$, and $f/f_0 = 1.5$.

filter. There is relatively good reflecting surface for 2.5D substrate (for $f \geq 0.6$ THz) compared with 2.2D and 2.0D. Figure 3 shows the behavior of the structure when the wave from varying dimension substrate is incident at different angles. Structure acts as a good reflecting surface for a wave from 2.0D substrate between 32° and 37° ($\approx 1\%$ parallel transmission power). In Figure 3(d) it is clear that the structure behaves as a polarization rotator in 15° – 35° and 40° – 90° region.

4.2. SC-SC Structure

As a second investigation, slabs placed at positions A and B are both made of SC MTM. Figure 4 illustrates the reflected and transmitted powers as a function of incident angle. Figures 4(a) and 4(b) show that there is no reflection at 25° for all substrates. However, wave from substrate 2.0D (solid line) has wider region of no reflection that is 23° – 27° . Figure 4(d) shows the maximum transmission at 22° . Parallel component of transmission is active in band 22° – 37° and has 70% of power transmission at 35° . Relation of reflected and transmitted powers with frequency at normal incidence for varying dimensions are depicted in Figure 5. At normal incidence, only parallel component of reflected wave exists ($R_\perp = 0$). Reflected power increases with the increase in dimension when the frequency is 0.5 THz and more. This structure produces bell-shaped reflecting bands. The maximum power reflected for 2.0D, 2.2D, and 2.5D is 60%, 77%, and 95%, respectively. In Figure 5(a), the maxima occur at 1.75 THz for all substrates. 2.0D wave has constant bands with reflection power of 61% and bandwidth of 0.25 THz (3 dB bandwidth) except that at odd harmonics it has 0.05 THz bandwidth, and reflection power is 13%. 2.2D and 2.5D waves have constant bands of 0.30 THz and 0.5 THz with reflection power of 88% and 99%, respectively (for higher values of f). In Figure 5(c), considering wave from 2.0D substrate, it is seen that parallel component of transmission is maximum at 1.57 THz with the bandwidth of 0.1 THz (3 dB bandwidth). Also transmission is greater than 95% at (0.85, 1.08 and 1.57) THz. Parallel transmission for 2.2D and 2.5D is maximum at 0.85 THz. This shows that the structure behaves like a narrow-band filter. The structure can also be used in polarization conversion devices. Figure 5(d)

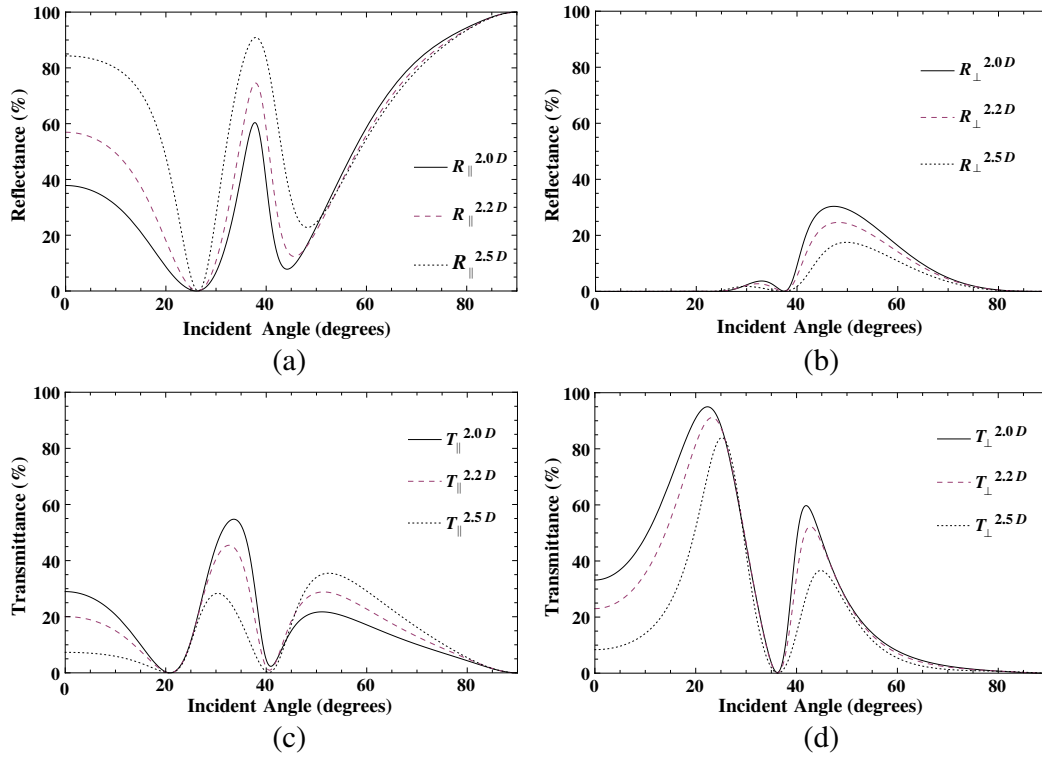


Figure 4. Reflectance and transmittance versus incident angle for five layered SC-SC structure. $n_A = 0.6$, $n_B = 0.458$, $\kappa_A = 1.0$, $\kappa_B = 0.76$, $|n_A|d_A = |n_B|d_B = \lambda_0/4$, and $f/f_0 = 1.5$.

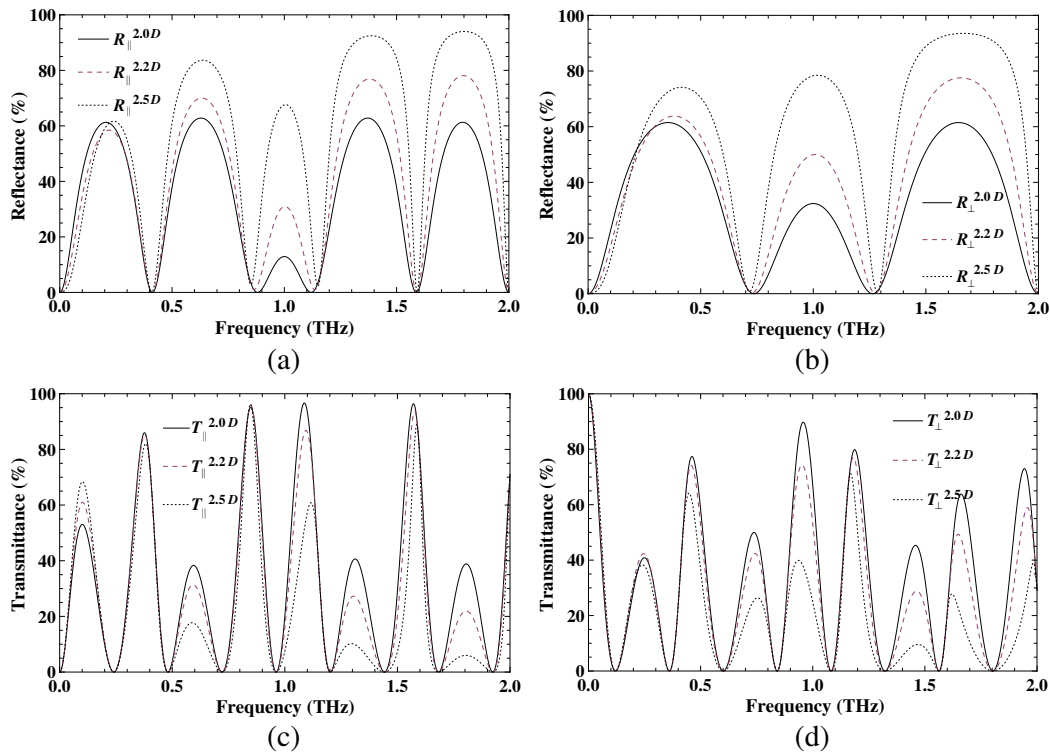


Figure 5. Reflectance and transmittance versus frequency for SC-SC structure. $n_A = 0.6$, $n_B = 0.458$, $\kappa_A = 1.0$, $\kappa_B = 0.76$, $|n_A|d_A = |n_B|d_B = \lambda_0/4$, and $\theta_i = 0^\circ$. (a) Five layered structure. (b) Three layered structure. (c) Five layered structure. (d) Five layered structure.

represents the existence of perpendicular component of transmission for normal incidence. Chirality introduces the optical activity in the structure thereby resulting in polarization conversion. Reflected power for three-layered SC-SC structure as a function of frequency is shown in Figure 5(b). It is seen that bandwidth and reflecting power of the structure are increased, i.e., the reflection bands are wider (spread). At this point, it is clear that the three-layered SC-SC structure forms higher reflection coating in 2.5D substrate than five-layered SC-SC structures.

4.3. SC-Dielectric Structure

As a third case, slab A remains the same as in previous case (SC MTM), and slab B is replaced with dielectric medium. To examine the behaviour of SC-dielectric structure in fractional space, reflection and transmission as a function of incident angle, frequency and chirality are shown in Figures 6 and 7. In Figure 6(a), when a wave from 2.2D substrate strikes SC-dielectric structure, it has zero reflection at 45° . Wave from 2.0D substrate has wider zero reflection region, which is from 38° – 50° . In this region, the structure can be characterise as an anti-reflection coating surface. Also, it can be used as reflection coating surface with varying power from 75% to 80% in the range 0° to 20° of incident angle. Figure 6(b) shows the perpendicular component of reflection. The maximum reflection is 25% at 70° when the wave is incident from 2.0D substrate. Figures 6(c) and 6(d) represent parallel and perpendicular transmission components versus angle of incidence. It is observed that parallel transmission power never increases more than 20% for any fractional dimension substrate. Perpendicular transmission component has a peak value of 92% at 44° for 2.0D and 2.2D, and it is 90% at 45° for 2.5D substrate. This shows that the structure can be used as high transmission coating surface around 45° incident angle, for all three substrates. The response of the structure for varying frequency, when the wave is normally incident upon it, is illustrated in Figure 7. As seen in Figure 7(a), the structure is a wideband frequency reject filter. Figure 7(d) depicts that the structure has the ability to behave as a narrow bandpass filter. Comparing both figures it is clear that at odd harmonics, the structure acts as high

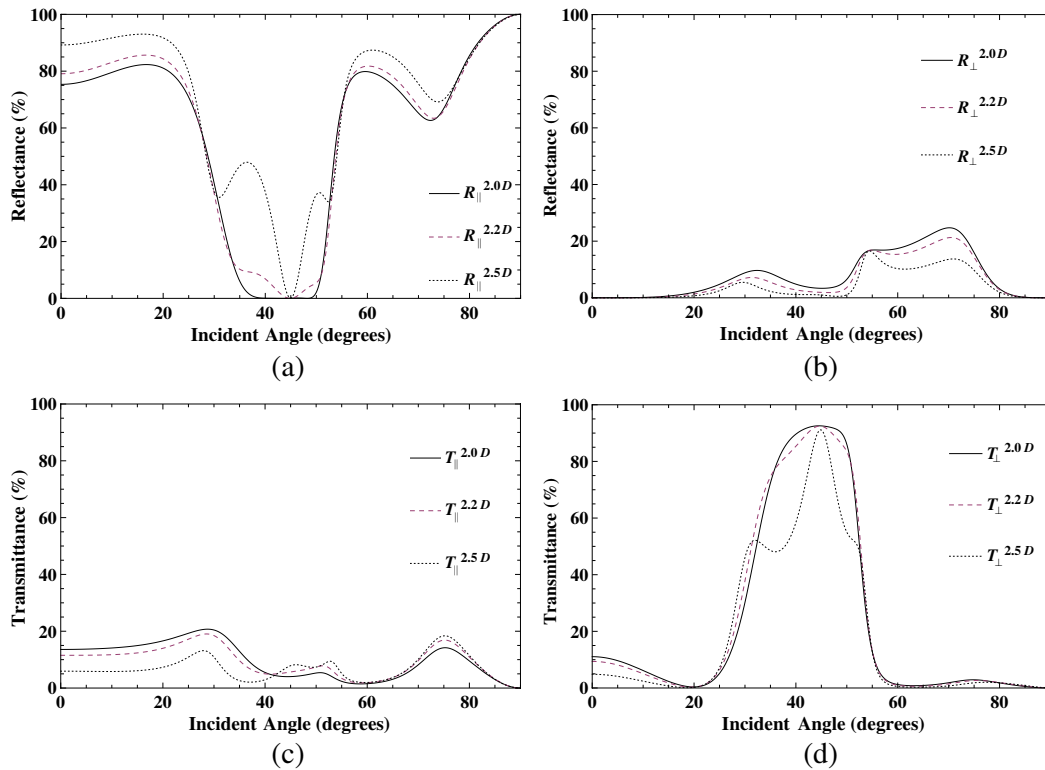


Figure 6. Reflectance and transmittance versus incident angle for SC-D structure. $n_A = 0.458$, $n_B = 2.2$, $\kappa_A = 0.76$, $\kappa_B = 0$, $|n_A|d_A = |n_B|d_B = \lambda_0/4$, and $f/f_0 = 1.5$.

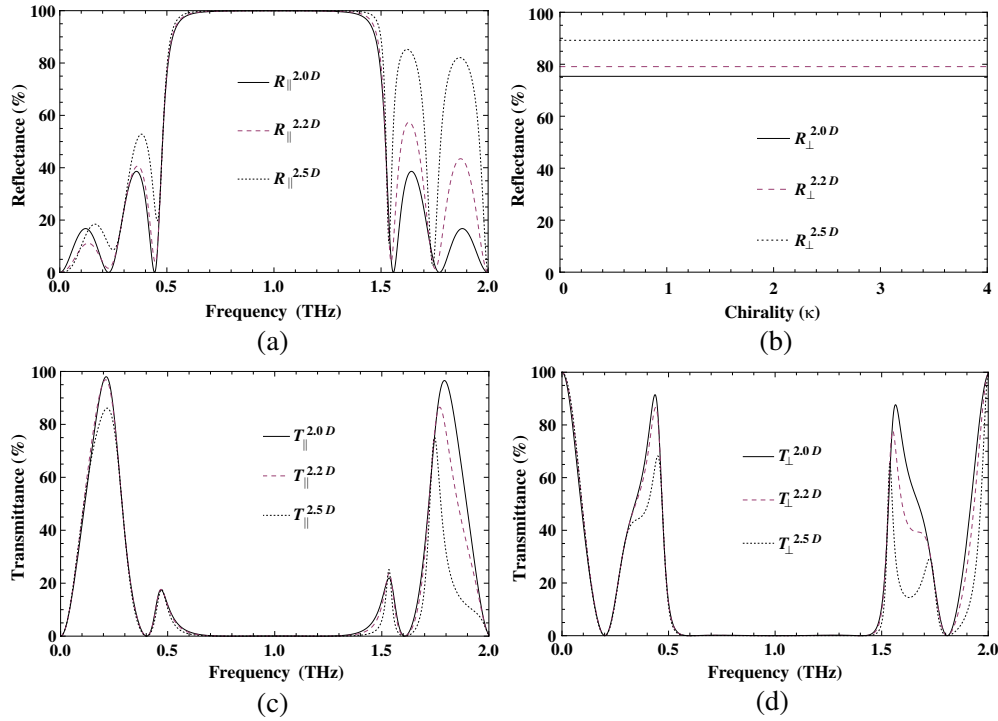


Figure 7. Reflectance and transmittance for SC-D structure. $n_A = 0.458$, $n_B = 2.2$, $\kappa_A = 0.76$, $\kappa_B = 0$, $|n_A|d_A = |n_B|d_B = \lambda_0/4$, and $\theta_i = 0^\circ$.

reflection coating (bandwidth ≈ 1.0 THz), and at even harmonics, it acts as narrow bandpass (anti-reflection/high transmission coating) filter. Note that for normally incident wave, the structure has an active perpendicular transmission component. This means that it can also be used in polarization conversion devices. Figure 7(b) shows the variation of reflected power for different dimensions when chirality of slab A is varied at frequency 1.5 THz. Increase in dimension results in increase in reflected power at a specific chirality value for $\theta_i = 0$.

4.4. CN-CN Structure

As a fourth case, both slabs of the structure are now composed of CN MTM. It is observed that the structure behaves like a high reflection coating for wider range of frequency as shown in Figure 8. The reflected power is 100% from 2 THz onwards. In Figure 8(b), there is a small window of transmission at lower frequencies (≤ 0.4 THz).

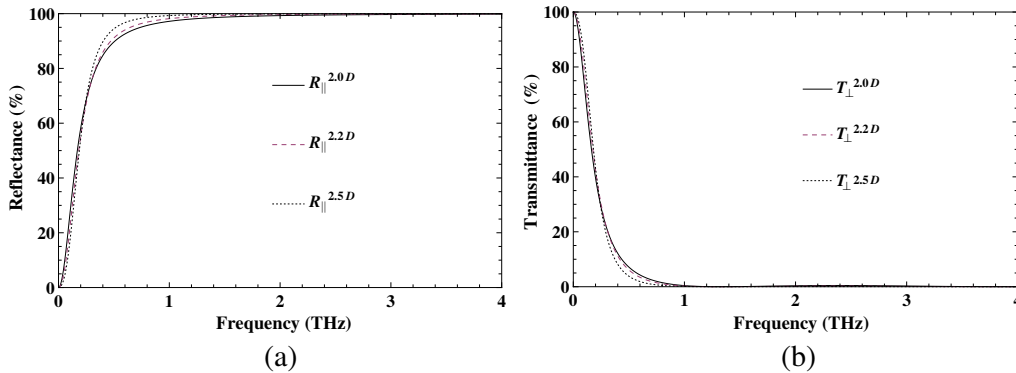


Figure 8. Reflectance and transmittance versus frequency for five layered CN-CN structure. $n_A = 2 \times 10^{-3}$, $n_B = 6 \times 10^{-3}$, $\kappa_A = \kappa_B = 0.25$, $d_A = d_B = \lambda_0/4$. (a), (b) Normal incidence.

5. CONCLUSION

In this paper, a solution for reflection and transmission from multilayered metamaterial structures sandwiched between fractal medium (non-integer dimension) is formulated. The behaviors of the structures are analyzed by obtaining parallel and perpendicular modes as a function of dimension, frequency, angle of incidence and chirality. Effect of dimension (integer and non-integer) of substrate on reflected and transmitted power for a particular structure has been discussed in detail. Four investigations are presented in this paper, chiral-chiral, strong chiral-strong chiral, strong chiral-dielectric, and chiral nihility-chiral nihility. Moreover, these multilayered periodic structures are examined, and numerical results for varying frequency and incident angle are presented. All the results fulfill the law of power conservation. This work provides solution for examining the electromagnetic fields and waves in multilayered structures in fractional dimension space. Also it paves path to investigate slabs and waveguide filled with fractal medium.

REFERENCES

1. Oraizi, H. and A. Abdolali, "Design and optimization of planar multilayer antireflection metamaterial coatings at ku band under circularly polarized oblique plane wave incidence," *Progress In Electromagnetics Research C*, Vol. 3, 1–18, 2008.
2. Yuan, C. X., Z. X. Zhou, J. W. Zhang, X. Li Xiang, Y. Feng, and H. G. Sun, "Properties of propagation of electromagnetic wave in a multilayer radar-absorbing structure with plasma- and radar-absorbing material," *IEEE Transactions on Plasma Science*, Vol. 39, No. 9, 2011.
3. Oraizi, H. and M. Afsahi, "Design of metamaterial multilayer structures as frequency selective surfaces," *Progress In Electromagnetics Research C*, Vol. 6, 115–126, 2009.
4. Sabah, C., H. T. Tastan, F. Dincer, K. Delihacioglu, M. Karaaslan, and E. Unal, "Transmission tunneling through the multilayer double-negative and double-positive slabs," *Progress In Electromagnetics Research*, Vol. 138, 293–306, 2013.
5. Liu, C. H. and N. Behdad, "Tunneling and filtering characteristics of cascaded-negative metamaterial layers sandwiched by doublepositive layers," *Journal of Applied Physics*, Vol. 111, No. 1, 014906–014906-9, 2012.
6. Sabah, C. and S. Uckun, "Multilayer system of Lorentz/Drude type metamaterials with dielectric slabs and its application to electromagnetic filters," *Progress In Electromagnetics Research*, Vol. 91, 349–364, 2009.
7. Demmie, P. N. and M. Ostojca-Starzewski, "Waves in fractal media," *Journal of Elasticity*, Vol. 104, No. 1–2, 187–204, 2011.
8. Mandelbrot, B., *The Fractal Geometry of Nature*, Freeman, New York, 1982.
9. Barnsley, M. F., *Fractals Everywhere*, Morgan Kaufmann, San Mateo, 1993.
10. Zubair, M., M. J. Mughal, and Q. A. Naqvi, "The wave equation and general plane wave solutions in fractional space," *Progress In Electromagnetics Research Letters*, Vol. 19, 137–146, 2010.
11. Zubair, M., M. J. Mughal, Q. A. Naqvi, and A. A. Rizvi, "Differential electromagnetic equations in fractional space," *Progress In Electromagnetics Research*, Vol. 114, 255–269, 2011.
12. Zubair, M., M. J. Mughal, and Q. A. Naqvi, "An exact solution of the cylindrical wave equation for electromagnetic field in fractional dimensional space," *Progress In Electromagnetics Research*, Vol. 114, 443–455, 2011.
13. Zubair, M., M. J. Mughal, and Q. A. Naqvi, "On electromagnetic wave propagation in fractional space," *Nonlinear Analysis B: Real World Applications*, Vol. 12, No. 5, 2844–2850, 2011.
14. Omar, M. and M. J. Mughal, "Behavior of electromagnetic waves at dielectric fractal-fractal interface in fractional spaces," *Progress In Electromagnetics Research M*, Vol. 28, 229–244, 2013.
15. Asad, H., M. Zubair, and M. J. Mughal, "Reflection and transmission at dielectric-fractal interface," *Progress In Electromagnetics Research*, Vol. 125, 543–558, 2012.

16. Asad, H., M. Zubair, M. J. Mughal, and Q. A. Naqvi, "Electromagnetic green functions for fractional space," *Journal of Electromagnetic Wave and Application*, Vol. 26, Nos. 14–15, 1903–1910, 2012.
17. Khan, S., A. Noor, and M. J. Mughal, "General solution for waveguide modes in fractional space," *Progress In Electromagnetics Research M*, Vol. 33, 105–120, 2013.
18. Khan, S. and M. J. Mughal, "General solution for TEM, TE, and TM waves in fractional dimensional space and its application in rectangular waveguide filled with fractional space," *Journal of Electromagnetic Waves and Applications*, Vol. 27, No. 18, 2298–2307, 2013.
19. Attiya, A. M., "Reflection and transmission of electromagnetic wave due to a quasi-fractional space slab," *Progress In Electromagnetics Research Letters*, Vol. 24, 119–128, 2011.
20. Ali, M., M. J. Mughal, A. A. Rahim, and Q. A. Naqvi, "The guided waves in planar waveguide partially filled with strong chiral material," *International Journal of Applied Electromagnetics and Mechanics*, Vol. 38, 139–149, 2012.
21. Shah, N. A., F. Ahmad, A. A. Syed, and Q. A. Naqvi, "Effects on reflected and transmitted powers of planar stratified structures involving chiral nihility meta-materials," *Journal of Applied Electromagnetics and Mechanics*, JAE1724, 2013.
22. Bassiri, S., C. H. Papas, and N. Engheta, "Electromagnetic wave propagation through a dielectric-chiral interface and through a chiral slab," *Journal of Optical Society of America*, Vol. 5, 1450–1459, 1988.
23. Mughal, M. J., M. M. Ali, and A. A. Rahim, "Analytical solution for electromagnetic resonance in strong chiral filled spherical cavity," *2012 IEEE Symposium Wireless Technology and Applications (ISWTA)*, 224–228, 2012.